J. Mt. Sci. (2017) 14(9): 1712-1727 e-mail: jms@imde.ac.cn http://jms.imde.ac.cn
https://doi.org/10.1007/s11629-017-4375-1

Debris flow susceptibility analysis based on the combined impacts of antecedent earthquakes and droughts: a case study for cascade hydropower stations in the upper Yangtze River, China

HU Gui-sheng [1] http://orcid.org/0000-0003-3378-2232; e-mail: huguisheng@imde.ac.cn

CHEN Ning-sheng [1*] http://orcid.org/0000-0002-6135-0739; e-mail: chennsh@imde.ac.cn

TANOLI Javed Iqbal [1,2] http://orcid.org/0000-0000-5409-2607; e-mail: javedtanoli@gmail.com

LIU Mei [1] http://orcid.org/0000-0001-8121-5772; e-mail: lmeimei90@163.com

LIU Rong-Kun [3] http://orcid.org/0000-0002-5911-6775; e-mail: cotineliu@qq.com

CHEN Kun-Ting [1] http://orcid.org/0000-0002-5982-822X; e-mail: kuntingchen@gmail.com

**Corresponding author*

1 *Key Lab of Mountain Hazards and Surface Processes, Institute of Mountain Hazards and Environment, Chinese Academy of Sciences, Chengdu 610041, China*

2 *Department of Earth Sciences, COMSATS Institute of Information Technology, Abbottabad 22060, Pakistan*

3 *School of Environment and Natural Resources, The Ohio State University, Columbus, OH, 43210, USA*

Citation: Hu GS, Chen NS, Tanoli JI, et al. (2017) Debris flow susceptibility analysis based on the combined impacts of antecedent earthquakes and droughts: a case study for cascade hydropower stations in the upper Yangtze River, China. Journal of Mountain Science 14(9). https://doi.org/10.1007/s11629-017-4375-1

Abstract: The upper Yangtze River region is one of the most frequent debris flow areas in China. The study area contains a cascade of six large hydropower stations located along the river with total capacity of more than 70 million kilowatts. The purpose of the study was to determine potential and dynamic differences in debris flow susceptibility and intensity with regard to seasonal monsoon events. We analyzed this region's debris flow history by examining the effective peak acceleration of antecedent earthquakes, the impacts of antecedent droughts, the combined effects of earthquakes and droughts, with regard to topography, precipitation, and loose solid material conditions. Based on these factors, we developed a debris flow susceptibility map. Results indicate that the entire debris flow susceptibility area is 167,500 km^2, of which 26,800 km^2 falls within the high susceptibility area, with 60,900 km^2 in medium and 79,800 km^2 are in low susceptibility areas. Three of the six large hydropower stations are located within the areas with high risk of debris flows. The synthetic zonation map of debris flow susceptibility for the study area corresponds with both the investigation data and actual distribution of debris flows. The results of debris flow susceptibility provide base-line data for mitigating, assessing, controlling and monitoring of debris flows hazards.

Keywords: Hydropower stations; Debris flow susceptibility; Earthquake; Drought; Geological Information System(GIS); Upper Yangtze River

Received: 18 January 2017
Revised: 27 February 2017
Accepted: 5 June 2017

Introduction

China is one of the countries which are severely and most frequently hit by debris-flow disasters. Debris flows occurred in about 31 provinces, cities and municipalities, and 950 counties, where there are more than 80 thousand debris flow gullies and 8,500 gullies which are potential debris flow triggering zones (Kang et al. 2004). The total active area is about 4.3×10^6 km^2, with more than 1.3×10^6 km^2 falling into the most potentially active category (Kang et al. 2004). About 50% of debris flow disasters in China are located in the upper Yangtze River region (Zhong et al. 2010). From 1753 to 2002, 17 super-large disastrous debris flows took place along the upper Yangtze River, each causing more than 100 casualties with an accumulated death toll of more than 6000 (Zhong et al. 2010). From 1990 to 2000, more than 60 cities and counties have been damaged by debris flows, and direct average economic loss amounts to RMB$ 1.5 billion (Xie et al. 2004; Liu 2004), imposing long lasting challenges for large populations scattered in mountain areas of the region.

The analysis of Debris Flow Susceptibility (DFS) is crucial for mitigating, assessing and controlling debris flow hazards (Dong et al. 2008). Although it is generally agreed that many factors such as topography and geomorphology, water and loose solid material affect the development of debris flows, key compounding control factors that trigger disastrous debris flows in mountain areas have not been thoroughly studied. In recent years some methods and models have been applied to analyze debris flow susceptibility (Carrara et al. 2008; Wang et al. 2014; Chen et al. 2015; Shi et al. 2015; Bregoli et al. 2015; Cama et al. 2017). For example, Geography Information System (GIS) technology has increasingly been used on debris flow susceptibility analysis and has greatly enhanced the ability to conduct spatial data processing and analysis (Mhaske and Choudhury 2010; Xu et al.2013; Kritikos and Davies 2015). However, the similarity of models which produce colorful debris flow susceptibility maps causes suspicion with regard to their validity (Dong et al. 2008) with many unresolved questions: are the causal factors selected in the statistically-based DFS model relevant for representing the occurrence of debris flow? How to complete early and dynamic analysis of DFS? Whether a new method can be applied for the analysis of DFS?

Many studies have shown that antecedent earthquakes, droughts and debris flows are closely related (Irmler et al. 2006; Zhu et al. 2011; Chen et al. 2014). The Chayu earthquake hit Tibet in 1950, and a large-scale debris flow triggered in Guxiang of Bomi County, Tibet in 1953. From then to now, intermittent outbreaks of very large, large, medium and small-scale debris flows have happened nearly 1000 times (Du 1985; Zhu et al. 1997; Liu 2003). Many studies have demonstrated that large amounts of loose solid material are the outcome of earthquakes (Li et al. 2008; Tang et al. 2009; Chen et al. 2014).

It usually takes three to five years from the generation of loose solid materials resulting from an earthquake to translate into an active debris flow (Du 1985; Liu 2003; Iverson et al. 2010). In recent years, several strong debris flow activities happened after some major earthquakes. For example, the frequency and scale of debris flows increased at the Chenyulan River basin in Nantou County in Taiwan in the two years following the 1999 Chi-Chi earthquake (Lin et al. 2004). The 2008 Wenchuan earthquake in China was followed by the outbreak of 72 debris flows in several earthquake disasters areas (Tang et al. 2009). In China, there are 23 earthquake zones, of which seventeen are active debris flow zones, accounting for more than 70% of the earthquake zones (Li et al. 2001). The Jiangjiagou gully in Southwest China has the highest debris flow frequency in the world and is located in the Xiaojiang earthquake fault zone (Du 1987; Wu et al. 1990). Similar examples can also be found around the world, for example, the Alaska debris flow in 1964 coupled well with the Alaska earthquake (Ryan et al. 2009).

Some surveys and studies have shown that there is an associated relationship between extremely arid climate and debris flows (Chen et al. 2014). Debris flow disasters in China are mainly distributed in Xinjiang, the Yellow River, and the Loess Plateau region, which are all semi-arid areas and sub-humid areas (Chen et al. 2014). Although some debris flows have occurred in wet years (Kessler et al. 2001), they are usually caused by very dry antecedent conditions before the wet seasons. In the watershed of Lake Braies in northern Italy, sediment deposition data for the last 4500 years show that debris flows are closely related to the seasonal extreme weather change (Irmler et al. 2006).

Based on an analysis of 116 disastrous debris flow events in China in the years 2010-2012, the data in China show a close relationship between debris flows and antecedent droughts (Chen et al. 2014). Debris flows in China during the last 100 years have occurred across a wide spectrum of climate types and landforms. It has been found that there is a combined impact of earthquakes and droughts on disastrous debris flows and it varies from low to very high according to different climate conditions and terrains. Research results show that in dry valleys of the upper reaches of the Yangtze River, the combined effects from both antecedent earthquakes and droughts on debris flows are significant (Chen et al. 2014). For instance, the Bailongjiang River basin has a seismic coupling rate of 91.7% and a drought coupling rate of 50%. Similarly, the Minjiang River basin has coupling rates of 87.5% and 50%, the upper reaches of Dadu River 88.9% and 50%, Jinsha River 100% and 60%, and the Xiaojiang River 87.5% and 60% (Chen et al. 2014).

In this research, we chose the cascade hydropower stations region in the upper Yangtze River as our case study area. We apply this method for the early and dynamic analysis of DFS on cascade hydropower stations region in the upper Yangtze River by analyzing the data of regional antecedent earthquakes and droughts on the basis of accordance with topography, precipitation and loose solid material conditions of debris flow triggering. The results of this study can provide an alternate methodology to study regional debris flow susceptibility, and supplies support for mitigating, assessing, controlling and monitoring debris flow risks for cascade hydropower stations.

1 Study Area

The upper Yangtze River is 4,500 km long, and its watershed area covers 1,005,400 km², accounting for 55.8% of the Yangtze River area. In recent years many large-size hydropower stations have been initiated along the upper Yangtze River region encompassing 200,000 km² with a north-south width of 100 km. The study area is rectangular in shape, having Yichang in Hubei Province on the east side and Lijiang in Yunnan Province on the west (Figure 1). The study area includes six large hydropower stations: Wudongde, Baihetan, Xiluodu, Xiangjiaba, Three Gorges and

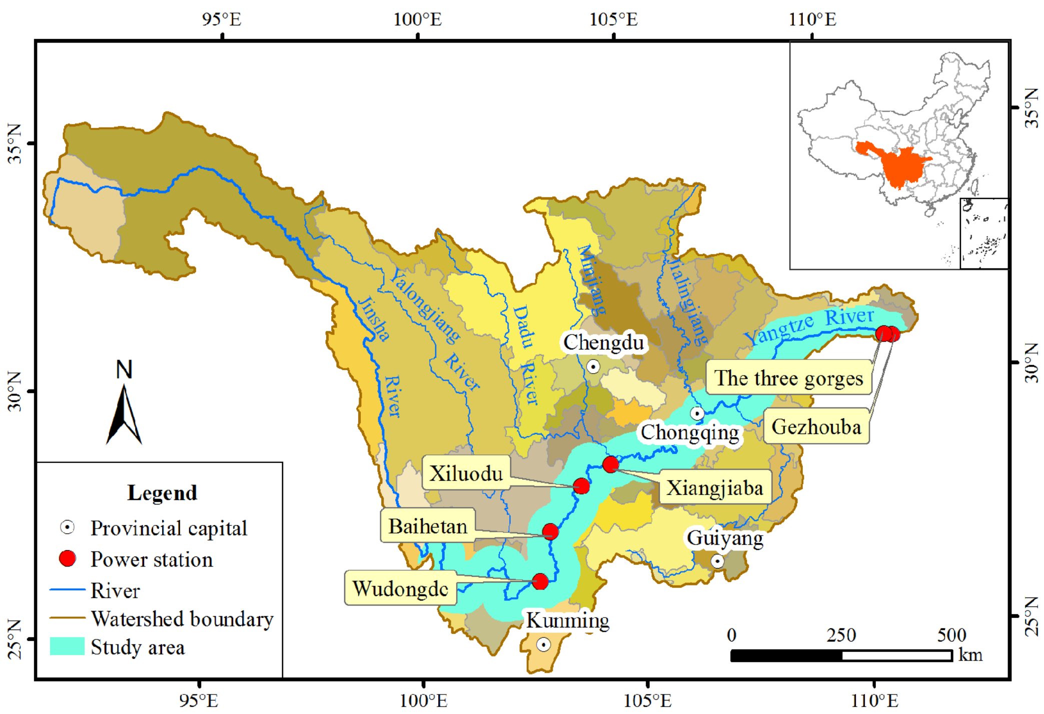

Figure 1 Location of study area of debris flow susceptibility.

Gezhouba. The total installed capacity of these hydropower stations is more than 70 million kilowatts. Several hydropower stations have been affected by disastrous debris flows during the construction and operational periods because of high terrain elevation difference, frequent earthquakes including more than 300 earthquakes since 2008 (Zhong et al. 2010), and intensive summer precipitation in the region. For example, nine large debris flow gullies broke out on 28 June, 2012, including at the Aizi gully where 41 people died or were missing at the Baihetan hydropower station (He et al. 2013).

The study area is located on a transitional zone between the first and second topographic terrace of China. Plateaus, basins and mountains are interlaced in the region. Sharp changes in terrain elevation can satisfy the basic topographical conditions of debris flow formation. The region has suffered several tectonic movements in geological history with a strong influence by Himalayan movement from Eocene to Pleistocene. The Himalayan movement has created and uplifted the Himalayas and Qinghai-Tibet Plateau and formed the first topographic terrace of China. At the same time, the interaction among the Eurasia, Pacific Ocean, and Indian plates has formed the second ladder due to differences of strong crustal movement during which the large quantities of loose solid material was generated (Ren et al. 1997).

Influenced by the Indian Ocean and Pacific Ocean airstreams, the southeast monsoon and southwest monsoon bring abundant precipitation to most parts of the study area. The abundant precipitation thus supplies favorable water conditions for debris flows to occur. Most parts of the study area are also under strong influence of human activities. Some human activities can aggravate the development of debris flows such as excessive forest clearance, intensified farming on steep slopes, extensive mountain road construction, and over mining (Wei et al. 2007). It is easy to trigger debris flows in the study area due to its various landforms, complex geological structures, abundant loose solid material, and heavy precipitation. In order to prevent and mitigate debris flow hazard in the cascade hydropower stations region, it is crucial to conduct early and dynamic analysis of debris flow susceptibility based on combined impacts of antecedent earthquakes and droughts before annual monsoonal precipitation arrives.

2 Methods

Remote sensing and geographic information system (GIS) technology has been successfully applied to more than one hundred technospheres of nine categories including resource management, automatic mapping, and regional planning (Cao and Hu 1993). After several decades of development, the susceptibility assessment methods of debris flows have advanced from qualitative to quantitative and from single to integrated (Wen et al. 2013; Kritikos and Davies 2015). Based on the conditions of topography, loose solid materials, hydrology, forest vegetation and human activities, these methods select several related indicators to reflect the susceptible degree of debris flows. However, the disaster prone environment has changed dramatically with time, making the susceptibility assessment of debris flows more complex and uncertain after earthquake and climate change (Wang et al. 2014).

Therefore, early and dynamic issues of debris flow susceptibility in mountainous area are a key issue to be addressed. A new method is proposed that takes into account the combined impacts of antecedent earthquakes and droughts. The existing research results show that the relationship between earthquakes and droughts and disastrous debris flows are significant in the upper Yangtze River region (Chen et al. 2014).

In our proposed method, the region's debris flow susceptibility is analyzed by examining the antecedent earthquakes effective peak acceleration, the impacts of antecedent droughts, and their combined effects on the study area on the basis of its relationship with topography, precipitation and loose solid material conditions of debris flow triggering in the region. The DFS of the study area can be analyzed by calculating antecedent earthquake Effective Peak Acceleration (EPA). The EPA is selected to assess the effects of seismic events on the study area, and combines impacts of both antecedent earthquakes and droughts. The map of DFS on the cascade hydropower stations region can be acquired based on GIS (Figure 2). The method is explained stepwise as follows:

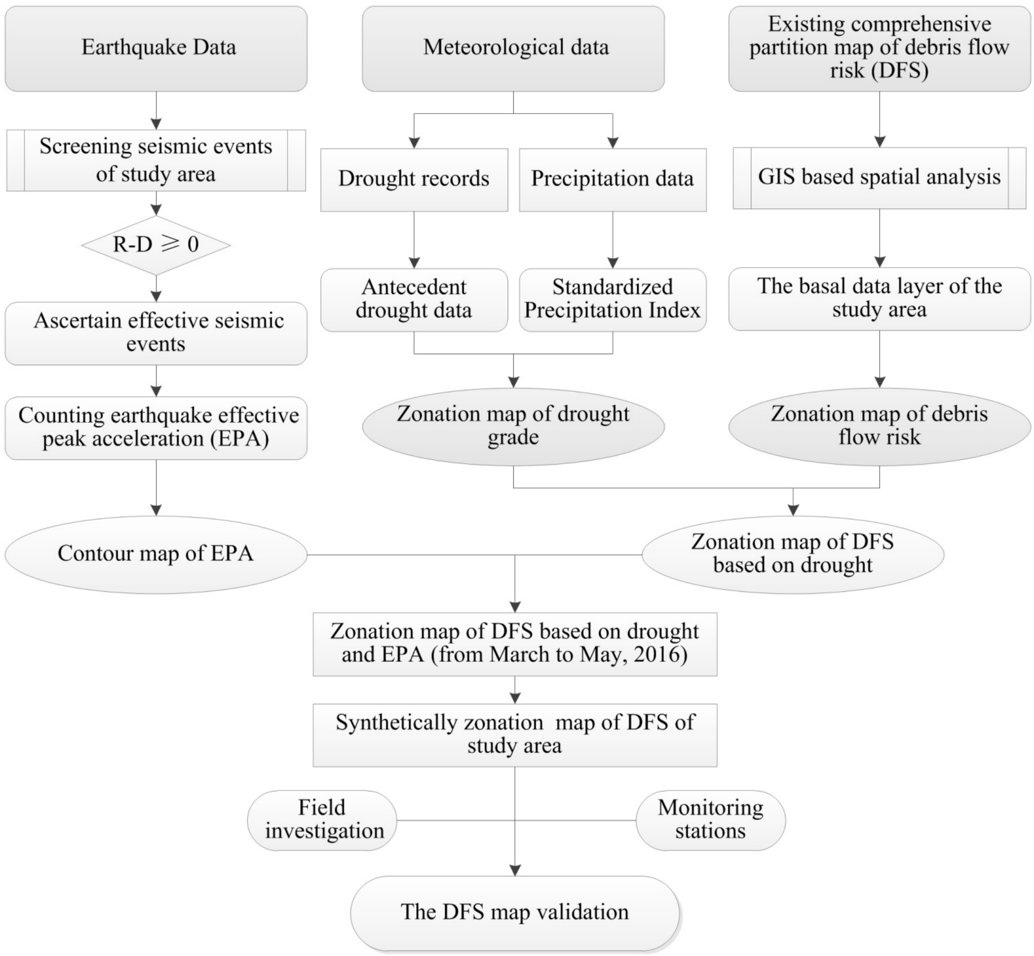

Figure 2 The logical flowchart of the methodological framework. EPA, Effective Peak Acceleration; DFS, Debris Flow Susceptibility.

(1) Screening seismic events in the upper Yangtze River region

Earthquake data for the last five years with a magnitude 4.5 or higher and the data for the last ten years with a magnitude 6 or higher are filtered based on seismic activity information from the China Earthquake Data Center (CEDC 2017). The inductive radius value R is counted based on the relationship between the sensible earthquake radius (R) and earthquake magnitude (M) (Wang and Shi 1993) by considering the magnitude M ≤ 5 ($R = 10^{-2.803+0.974M}$) and M ≥ 5 ($R = 10^{0.611+0.289M}$).

(2) Screening effective seismic events in the upper Yangtze River region

The distance (D) between a debris flow site and the earthquake epicenter is calculated by GIS. If R-D ≥ 0, the seismic events are assumed with effects on the debris flow sites, otherwise no effect is assumed.

(3) Counting earthquake effective peak acceleration

The EPA value is calculated by using the acceleration attenuation equation (Equation 1 to 3) (Yu and Gao 2001). The EPA value on the long axis (lw) and short axis (sw) is calculated separately by using Equation 1 and 2. The final EPA value, which is the geometric average between the EPA value of the long axis and short axis, is calculated by employing Equation 3.

$$EPA^{lw} = 10^{2.492+0.786M \quad 2.787\lg\left|d+3.269\exp(0.451M)\right|} \quad (1)$$

$$EPA^{sw} = 10^{1.093+0.591M \quad 1.794\lg\left|d+1.046\exp(0.451M)\right|} \quad (2)$$

$$EPA^{w} = \sqrt{EPA^{lw} \quad EPA^{sw}} \quad (3)$$

Where EPA^{W}, EPA^{sw} and EPA^{lw} are output variables, d and M are input variables. M is the magnitude, and d is the depth of epicenter (km).

(4) Production of the EPA contour map of antecedent earthquakes

The EPA value of each grid point

corresponding to these seismic points on the cascade hydropower stations region is calculated separately and overlaid. The EPA contour map of antecedent earthquakes on the cascade hydropower stations region was acquired according to the attenuation law of the EPA.

(5) Production of the map of drought grade on the study area

A distribution map of drought grade in China before the annual monsoon season was acquired from National Meteorological Information Center (NMIC 2017). A zonation map of drought on the study area is acquired by GIS.

(6) Production of the DFS distribution map

The contour map of earthquake influence was overlaid with the zonation map of DFS based on drought and comprehensive regionalization map of debris flow risk in the upper Yangtze River region by using GIS. The distribution map of DFS was produced based on drought and EPA data.

3 Analysis and Results

3.1 Extract the basal data layer of the study area

The Institute of Mountain Hazards and Environment, Chinese Academy of Sciences had already completed a comprehensive zonation map of debris flow risk based on the analysis of historical events of debris flow hazards, topography, geology, water and material in the upper Yangtze River region in 2001 (Zhong et al. 2010). The process of generating this comprehensive zonation map of debris flow risk is illustrated as follows (Han et al. 2007). Methodologies, historical and potential hazard degree were fully considered in the hazard assessment and a hazard index was presented to indicate the degree of debris flow hazards. Regarding the debris-flow vulnerability assessment, the statistical data and calculation procedure were based on hazard-degree regionalization instead of administrative divisions, which improved the assessment's precision. These quantitative methodologies integrated with GIS were applied for risk assessment of debris flows in the upper reaches of Yangtze River. These results provide references for debris-flow risk assessment and disaster management in the region.

However, this approach does not resolve early and dynamic issues of debris flow susceptibility due to differences of DFS with time. The basal data layer of the study area was extracted from the comprehensive zonation map of debris flow risk in the upper Yangtze River region by using GIS (Figure 3a). In order to correspond with classes of drought grade and EPA value, the zonation map of debris flow risk of the study area was divided into four zones: high danger, medium danger, low danger, no danger (Figure 3a). The highest and higher danger zones of figure 3a were re-classified as high grade, the medium danger zone of figure 3a was re-classified as medium grade, the mild and micro danger zone of figure 3a were re-classified as low grade, no debris flow of figure 3a was re-classified as no grade in the paper.

3.2 Analysis of overlay method by GIS

The method based on the analysis of debris flow influencing factors weights was most commonly used in superposition analysis (Macelloni et al. 2011; Kima et al. 2014; Yu et al. 2014). This method aims to accurately determine the weight of each influence factor (Tehrany et al. 2014; Veronesi et al. 2017). Research results show that the combined impacts from earthquakes and droughts on disastrous debris flows are significant in the upper Yangtze River region, and correlation coefficients of earthquakes and droughts with disastrous debris flows are almost equal (Chen et al. 2014). So weights of EPA value and drought grade are considered the same. Meanwhile, the analysis of DFS in the study area is based on the comprehensive zonation map of debris flow risk in 2001, and the weight of partition of debris flow risk in 2001 is determined as the same with EPA value and drought (Table 1 and Figure 3). The classes of drought grade, EPA value, debris flow risk and DFS of study area were divided into four including High,

Table 1 The weight value of debris flow susceptibility influencing factors

Weight	Factors		
	Partition of debris flow risk	Drought grade	EPA value
3	High (H)	High	High
2	Medium (M)	Medium	Medium
1	Low (L)	Low	Low
0	No (N)	No	No

Note: EPA is effective peak acceleration of earthquake.

Medium, Low and No in order to make it easier to overlay and analyze in GIS. It is defined that C is High when A and B are High, one of them is High and other is Medium. Similarly, it is defined that C is Low when A and B are Low, one of them is Medium and other is No, one of them is Low and other is No. It is certain that C is No when A and B are No. The C is Medium in addition to the above

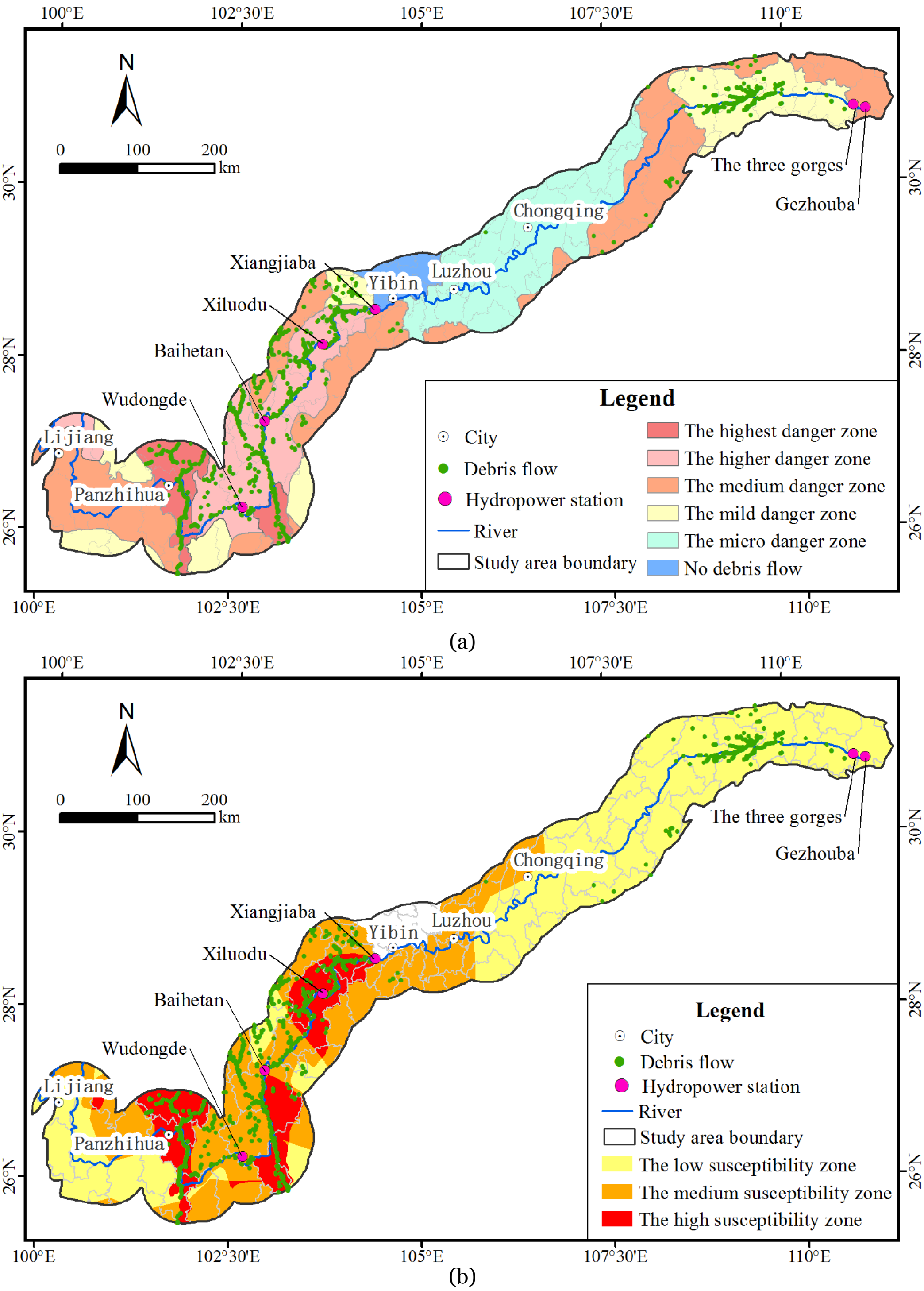

Figure 3 The zonation map of debris flow susceptibility based on drought (from March to May, 2016) for cascade hydropower stations. (a) the comprehensive zonation map of debris flow risk on the study area; (b) a zonation map of DFS based on drought data of March, 2016; (c) the partition result based on drought data of April, 2016; (d) the partition result based on drought data of May, 2016. (-To be continued-)

(-continued-)

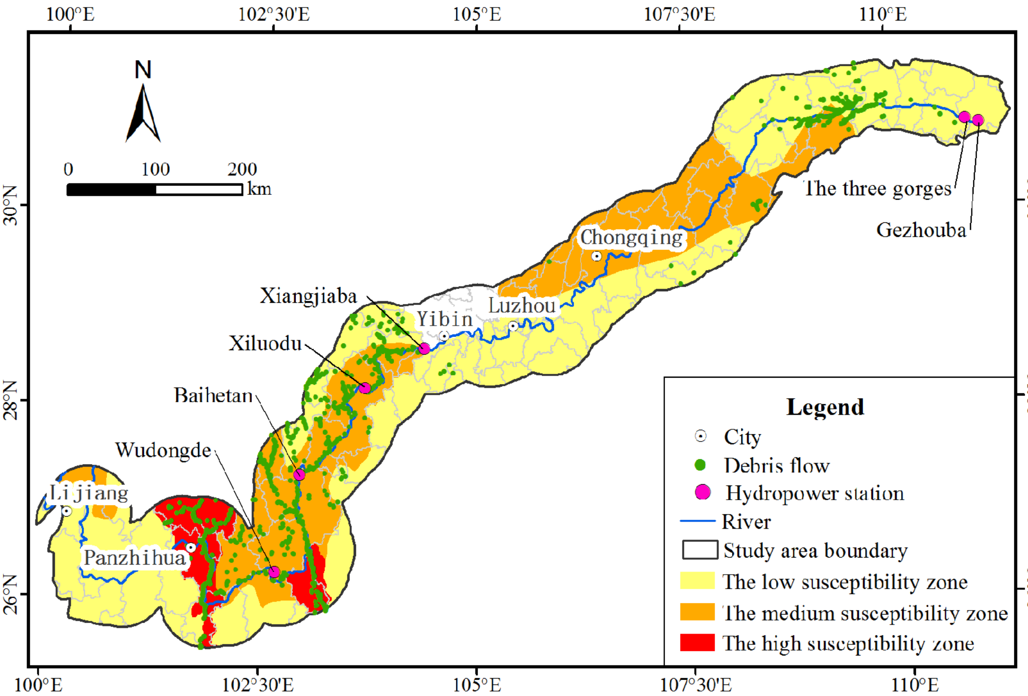

(c)

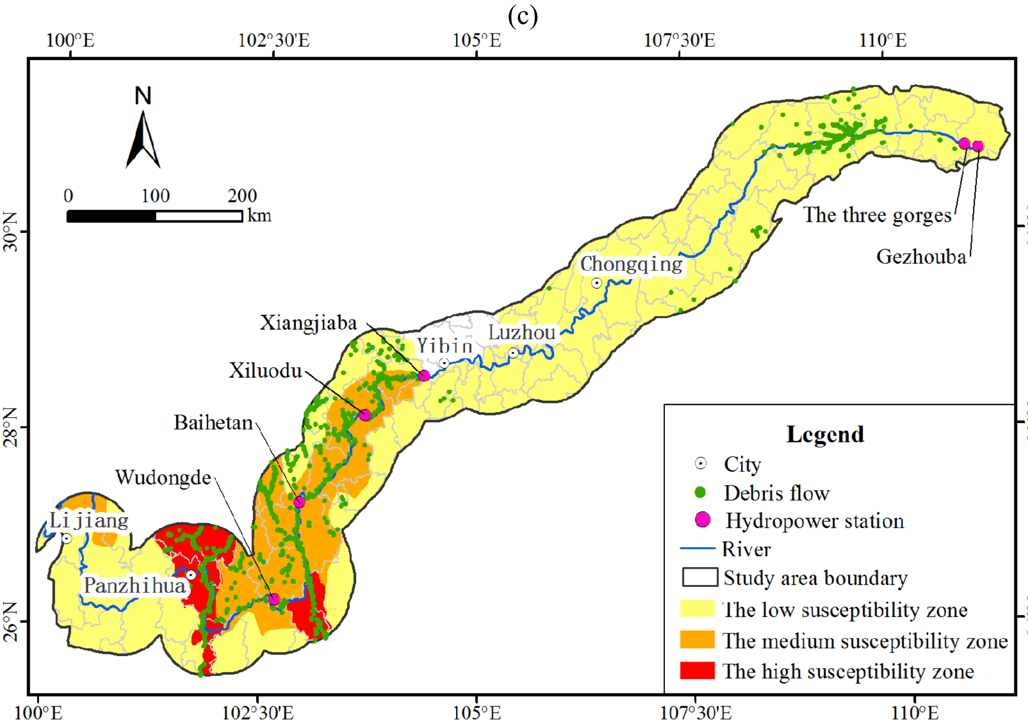

(d)

Figure 3 The zonation map of debris flow susceptibility based on drought (from March to May, 2016) for cascade hydropower stations. (a) the comprehensive zonation map of debris flow risk on the study area; (b) a zonation map of DFS based on drought data of March, 2016; (c) the partition result based on drought data of April, 2016; (d) the partition result based on drought data of May, 2016.

operation. When the overlay result is greater than or equal to the 2.5, the C is classified as High according the algorithms. When the overlay result is from 1.5 to 2.0, the C is classified as Medium. When the overlay result is from 0.5 to 1.0, the C is classified as Low.

3.3 Analysis of DFS based on drought

Proposed by McKee et al. (1993) the standard precipitation index (SPI) was used to divide the grade of drought events in selected areas in certain time. The SPI index is derived based on the rainfall data from the China Meteorological Administration Information Center (NMIC) in the area where debris flows broke out. Because of the differences in time and location, it is difficult to compare each area's precipitation. However, as the precipitation is skewed and not normally distributed, the precipitation analysis is therefore conducted by using the Gamma distribution and then the SPI values are obtained through the normal standardization. On the basis of the SPI index, droughts are classified into five groups (Fiorillo et al. 2012): SPI>-0.5 for the non-drought, -1<SPI≤-0.5 for light drought, and -1.5<SPI≤-1.0 for medium drought, -2.0<SPI≤-1.5 for severe drought, SPI≤-2.0 for extreme drought.

The drought grade from March to May, 2016 in the zonation map is divided into four zones: high drought (SPI≤-2.0), medium drought (-2.0<SPI≤-1.0), low drought (-1.0<SPI≤-0.5), and no-drought (SPI>-0.5). These four zones are overlaid with the comprehensive zonation map of debris flow risk (Figure 3a) of the upper Yangtze River region. A new zonation map of DFS based on drought data was generated as shown in Figures 3b, 3c, 3d.

3.4 DFS based on EPA of antecedent earthquakes

The DFS of the study area can be analyzed by calculating antecedent earthquakes' EPA. The detailed analysis process is explained stepwise as follows:

(1) Earthquake data

The antecedent earthquakes data of the study area were collected from the CEDC. The inductive radius value R was counted according to the relationship between inductive radius (R) and the magnitude (M) ($R=10^{-2.803+0.974M}$, M ≤ 5) and ($R=10^{0.611+0.289M}$, M ≥ 5) (Wang and Shi 1993).

(2) Screening effective seismic events of the study area

Firstly, the whole region of cascade hydropower stations in the upper Yangtze River (20,000km²) was divided into cells, with each cell being 10 km². The resulting 1,580 grid points of the study area were numbered from 0 to 1,579. Secondly, the distance (D) was counted between 105 seismic points (as shown in Table 2) for each grid point generated by using GIS, and comparing the results with the inductive radius (R). The seismic point is effective if R is greater than D between the seismic point and the grid point. Finally, effective events are filtered based on the above calculation (Table 2).

(3) The EPA contour map on the study area

The EPA value of each grid point (0-1579) corresponding to 31 seismic points on the cascade hydropower stations area is calculated separately by Equation 1 to 3, and the total EPA value for each grid point on the study area is acquired by superposition. The result is shown in Figure 4a.

3.5 Results of DFS on cascade hydropower stations development zone

The zonation map of DFS on the cascade hydropower stations development zone between March and May, 2016 was prepared by overlaying the EPA contour map on the zonation map of DFS based on drought (Figure 4b, 4c, 4d). The final zonation map of DFS on cascade hydropower stations development zone was finalized by overlaying the Figure 4b, 4c, 4d by using GIS. The result is shown in Figure 5.

This research shows that the entire susceptibility area of debris flow is 167,500km², of which 26,800 km² (16%) are considered as high susceptibility areas, whereas 60,900 km² (36%) and 79,800 km² (48%) are medium and low susceptibility areas, respectively. The high susceptibility areas of debris flow are mainly concentrated in the southwest of Sichuan Province and northwest Yunnan Province. The detailed distribution characteristics of the susceptibility areas of debris flow are from Yanbian and Panzhihua (Sichuan Province) to Luquan and Yuanmou (Yunnan Province), Ningnan (Sichuan Province) to Qiaojia and Huize (Yunnan Province), Suijiang (Yunnan Province) to Leibo (Sichuan Province), and the eastern region of Lijiang (Yunnan Province). In addition, the medium susceptibility areas of debris flow are mainly concentrated in the surrounding areas of Yibing, Luzhou, Huidong and Huili (Sichuan Province).

Both the left and right banks of the Wudongde hydropower station dam are in the medium debris flow susceptibility areas whereas both banks of the Baihetan hydropower station dam are in the high debris flow susceptibility areas. The whole region from the Baihetan hydropower station to the Wudongde hydropower station is in high susceptibility areas.

4 DFS Map Validation and Conclusions

4.1 Validation of case study

In order to verify the accuracy and reliability of research results, the Aizi gully of study area was chosen as a case study. Hazard process and triggering factors of "6.28" Aizi gully debris flow were analyzed and a relationship between Aizi gully debris flow and earthquakes & droughts have been revealed. Meanwhile, some automatic stations have been placed on the study area and debris flows field investigation was carried out in order to verify the results of the DFS.

4.1.1 Background of Aizi gully

The Aizi gully with a catchment area of 65.55 km^2 is located on the left bank of Jinsha River and south slope of Daliang Mountain (Figure 6), climatically falling in subtropical monsoon climate zone, with distinct dry and wet season. The length of the main stream is 21.96km, with a gradient of 155‰. In Aizi gully watershed, the highest point is

Table 2 Effective seismic events of cascade hydropower stations

No	Date	N (°)	E (°)	d (km)	M	Site	R (km)
				$4.5 \le M < 5$			
1	2013-2-19	28.35	104.84	10	4.5	Gongxian County, Sichuan Province	26.73
2	2012-6-12	28.1	104.28	9	4.5	Yanjing County, Yunnan Province	26.73
3	2011-4-15	26.66	102.94	12	4.5	Huidong County, Sichuan Province	26.73
4	2011-2-12	27.14	103.01	12	4.5	Qiaojia County, Yunnan Province	26.73
5	2010-9-10	29.36	105.43	6	4.5	Sichuan Province	26.73
6	2013-10-14	27.97	102.78	18	4.6	Zhaojue County, Sichuan Province	33.19
7	2013-4-25	28.4	104.95	10	4.8	Changning County, Sichuan Province	51.17
8	2014-12-7	23.3	100.51	16	4.8	Jinggu County, Yunnan Province	51.17
9	2013-2-19	27.1	103.1	10	4.9	Qiaojia County, Yunnan Province	63.53
10	2010-8-29	27.13	103.02	10	4.9	Yunnan Province	63.53
				$5 \le M < 6$			
11	2015-1-14	29.3	103.2	20	5.0	Jinkouhe County, Sichuan Province	113.76
12	2014-4-5	28.14	103.57	13	5.1	Yongshan County, Yunnan Province	121.59
13	2010-2-25	25.42	101.94	20	5.2	Yunnan Province	129.96
14	2014-8-17	28.12	103.51	7	5.2	Yongshan County, Yunnan Province	129.96
15	2012-9-7	27.56	104.03	14	5.6	Yiliang County, Yunnan Province	169.59
16	2012-9-7	27.51	103.97	14	5.7	Yiliang County, Yunnan Province	181.26
17	2012-6-24	27.71	100.69	11	5.7	Ningliang County, Yunnan Province	181.26
18	2014-12-6	23.33	100.5	10	5.9	Jinggu County, Yunnan Province	207.06
19	2014-11-25	30.2	101.75	16	5.9	Kangding County, Sichuan Province	207.06
				$M \ge 6$			
20	2008-5-13	30.95	103.42	14	6.1	Sichuan Province	236.54
21	2008-5-12	31.27	103.82	14	6.3	Sichuan Province	270.21
22	2008-5-12	31.26	103.67	14	6.3	Sichuan Province	270.21
23	2008-8-30	26.3	102.06	19	6.3	Sichuan Province	270.21
24	2009-7-9	25.6	101.03	6	6.3	Yunnan Province	270.21
25	2008-5-25	32.55	105.48	14	6.4	Sichuan Province	288.8
26	2014-11-22	30.29	101.68	20	6.4	Kangding County, Sichuan Province	288.8
27	2008-8-5	32.72	105.61	13	6.5	Sichuan Province	308.67
28	2014-8-3	27.11	103.33	10	6.6	Ludian County, Yunna Province	329.91
29	2014-10-7	23.4	100.55	10	6.9	Jinggu County, Yunnan Province	402.81
30	2013-4-20	30.3	103.02	13	7.0	Lushan County, Sichuan Province	430.53
31	2008-5-12	31.01	103.42	14	8.0	Sichuan Province	837.53

Notes: N is latitude (°), E is longitude (°), d is depth of epicenter (km), M is the magnitude and R is inductive radius (km).

3646m while the lowest is 604m.The mean annual temperature is 19.0°C and mean annual precipitation is 960.5mm.There are two faults in the Aizi gully watershed: the Rossi and Huixiluohe faults; seismic activity is frequent in the fault zones (He et al. 2013). There are 10 villages in Aizi gully watershed with a total population of 577. The debris flow hazards site is located in the Baihetan

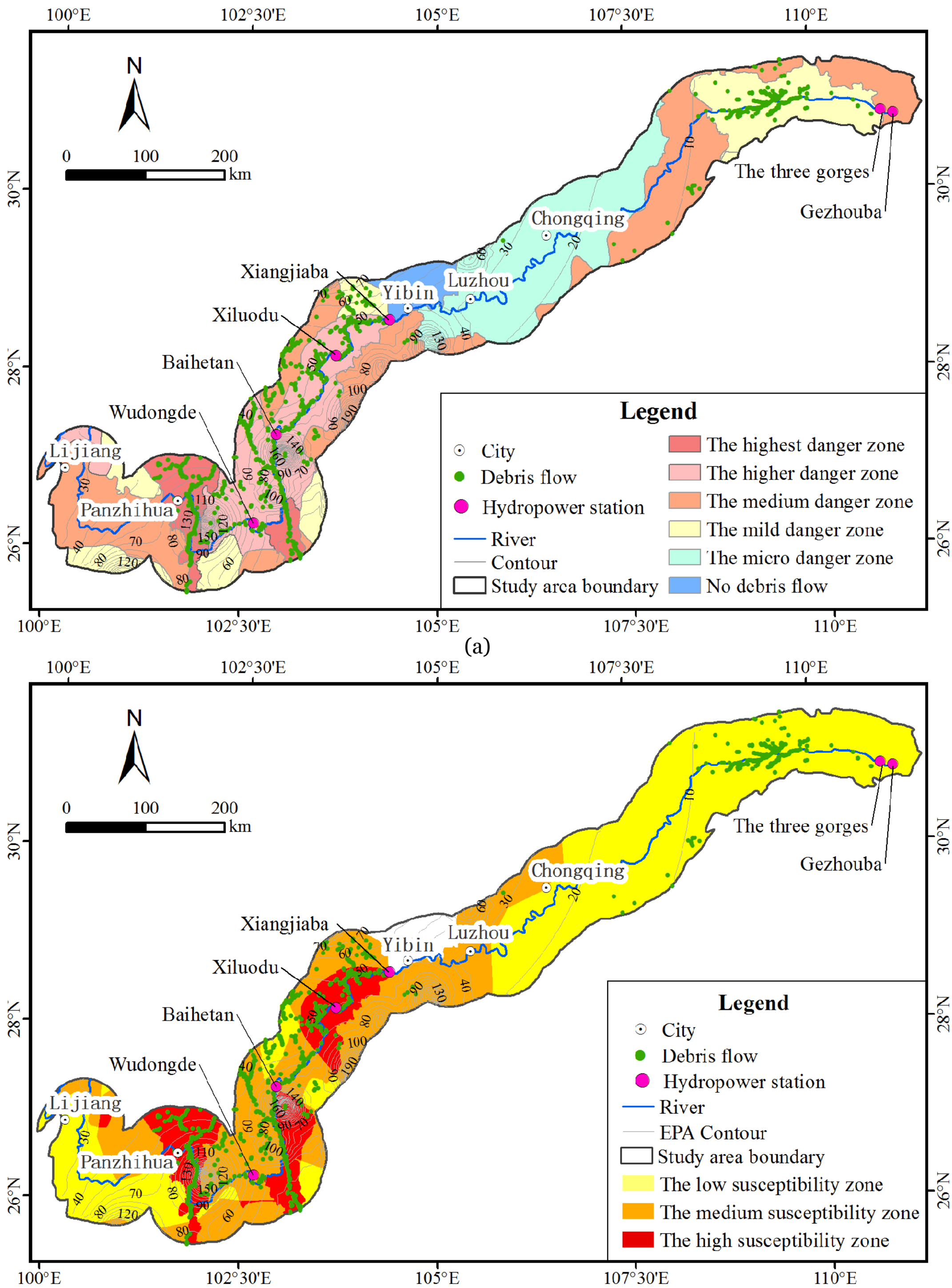

Figure 4 Zonation map of debris flow susceptibility based on drought and EPA (from March to May, 2016) for cascade hydropower stations. (a) is the contour map of EPA on the study area; (b), (c,) (d) are zonation maps of DFS on the study area based on drought and EPA from March to May, 2016, respectively) (-To be continued-)

(-continued-)

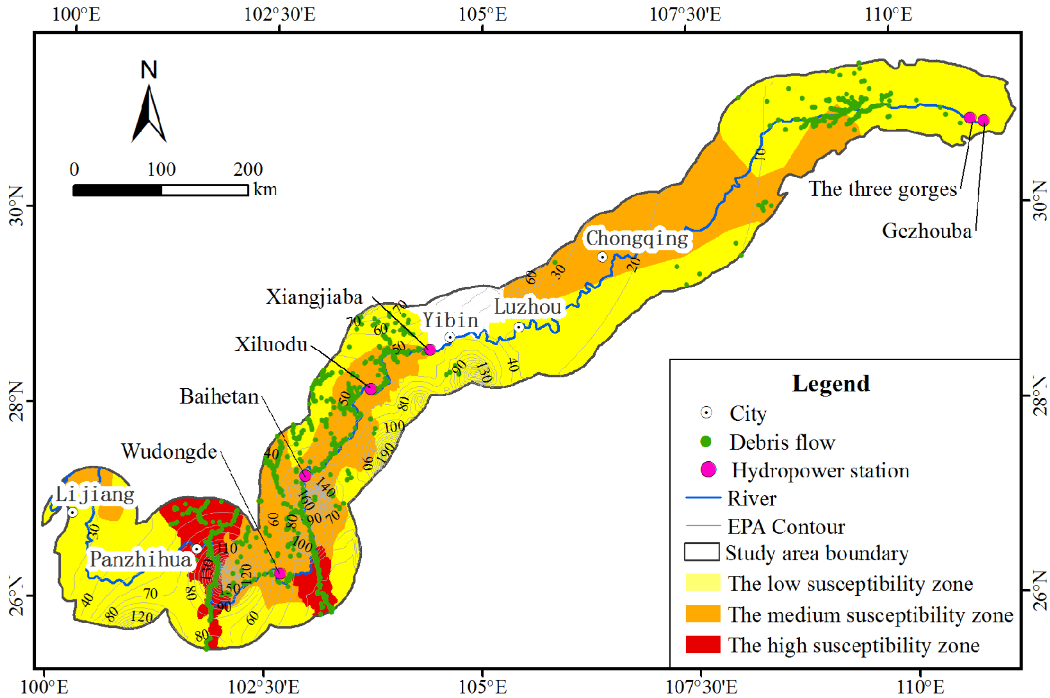

(c)

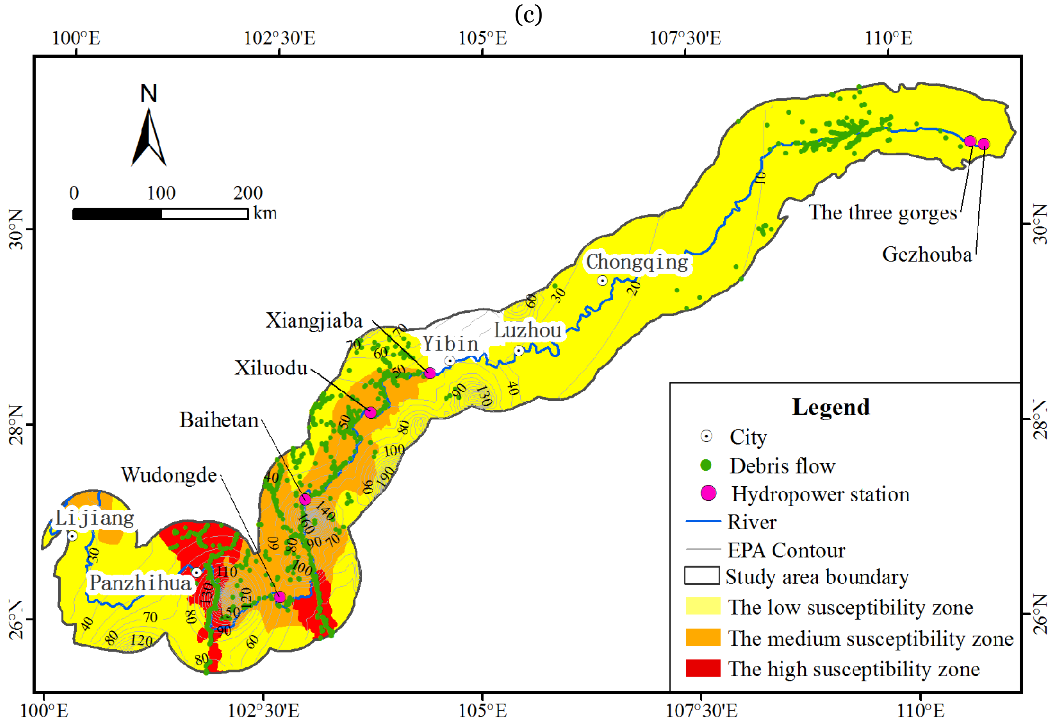

(d)

Figure 4 Zonation map of debris flow susceptibility based on drought and EPA (from March to May, 2016) for cascade hydropower stations. (a) is the contour map of EPA on the study area; (b), (c,) (d) are zonation maps of DFS on the study area based on drought and EPA from March to May, 2016, respectively).

hydropower project area (15 million KW) upstream of Yangtze River, a part of the Qinghai-Tibet Plateau earthquake zone. In a dry-hot valley, it is the second largest hydropower station in China.

4.1.2 Hazard process and triggering factors of "6.28" Aizi gully debris flow

On June 28, 2012, a large debris flow disaster

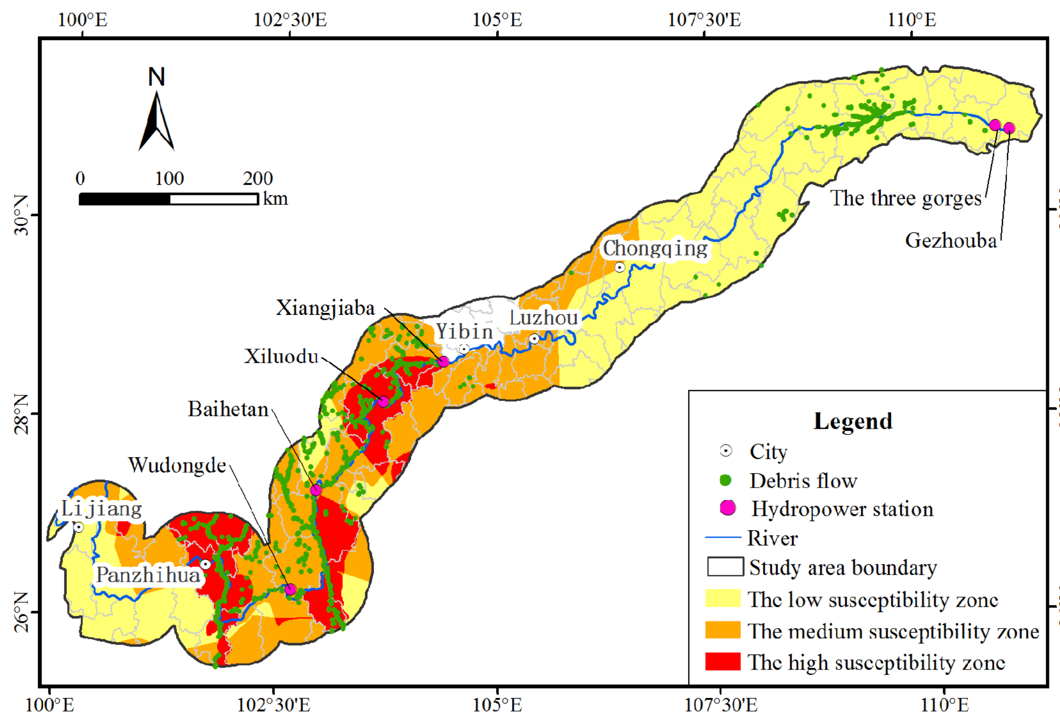

Figure 5 The synthetically zonation map of debris flow susceptibility for cascade hydropower stations.

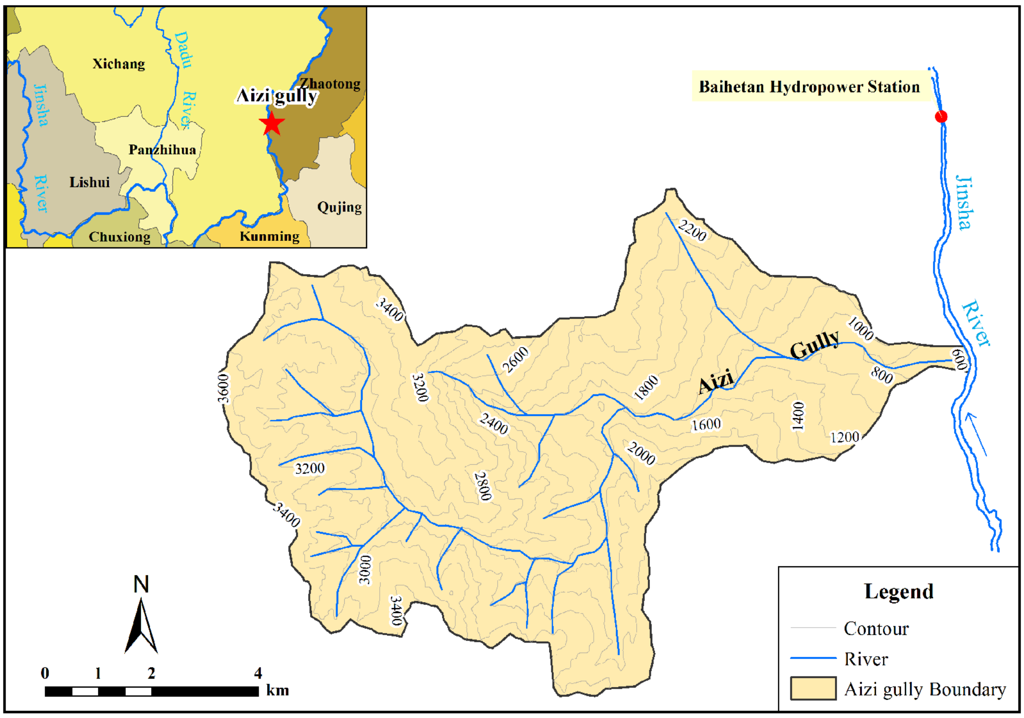

Figure 6 The location of the Aizi gully on cascade hydropower stations in the upper Yangtze River.

occurred in Aizi gully, Ningnan County, Sichuan province, China. This was the most severe disaster at a construction site in 2012 in China it resulted in 41 people dead or missing (Hu et al. 2014). Three triggering factors of the "6.28" Aizi gully debris flow can be categorized: (i) Aizi gully is located on the Zemuhe seismic zone, so the impact of earthquake on Aizi gully is obvious. From 1993 to 2012 the total number of earthquakes with magnitude more than 4.7 on Richter scale that affected the Aizi Valley is 16. From 2008 to 2012 there are five earthquakes that affected Aizi gully which provided abundant loose solid materials for the outbreak of the "6·28" debris flow. (ii) Ningnan County suffered drought for three consecutive years in 2009, 2010 and 2011. In 2012 Ningnan County suffered the worst drought in a century. Successive droughts in the recent years made the rock mass fragile and worsen the soil structure which can also provide abundant unconsolidated materials. (iii) Abundant antecedent rainfall followed by intense rainfall on June 28 plays an inducing role in debris flow formation. The hourly rainfall data was collected from June 27 to June 28, 2012 in Baihetan meteorological station and Xintian meteorological station, the largest rainfall occurred between 03:00 and 07:00 on June 28. The cumulative rainfall in these five hours reached 66.1mm, the mean rainfall intensity in this period was 13.2mm/h, and the maximum rainfall intensity was 23.3mm/h, which is much higher than the critical rainfall intensity 5mm/h (Chen et al. 2009). Rainfall discrepancy is notable in Aizi gully, and point rainstorm is mainly concentrated in its tributary with abundant loose materials first initiated slope debris flow in this tributary.

4.1.3 The relationship between Aizi gully debris flow and earthquakes & droughts

A long drought period which lasted around three years took place from the winter of 2009 to the spring of 2012 in the midstream of the Jinshajiang River where the Baihetan hydropower station and the Aizi valley are located. Amongst varied dynamic parameters that affect debris flows, earthquake and extreme drought are chosen to forecast debris flows since the basin was also affected by earthquake activity with GPA over 50gal in 2009. According to previous research results (Chen et al. 2014), droughts are likely to cause an increased looseness of solid mass and a decreased chance of debris flows triggered by significant rainfall. The basin was predicted to have a large scale debris flow in 2012 (Chen et al. 2010), and as predicted, a large scale debris flow was triggered at 5 am on June 28, 2012.

4.1.4 Validation of results

In order to verify the results of DFS on cascade hydropower stations development zone in the upper Yangtze River, eight automatic rainfall stations, four mud level sensors, four pore pressure sensors and four water potential sensors were placed in Aizi gully and Dazhai gully near the Baihetan hydropower station, and four automatic rainfall stations, two mud level sensors, two pore pressure sensors and two water potential sensors were placed in Huashan gully and Baitan gully near the Wudongde hydropower station. The startup and formation process of debris flow can be monitored by these automatic stations. On July 7, 2016 a debris flow was triggered in Aizi gully according to monitoring results of automatic stations in Baihetan hydropower station. In order to further verify the results of the study, we carried out a debris flow field investigation, and found some disastrous debris flows in the study area. For example, on September 17, 2016 two debris flows were triggered in Yuanmou county, Yunnan province and interrupted the120km-long highway. On September 20, 2016 another debris flow was triggered in Panzhihua city of Sichuan province, and the Beijing-Kunming highway was interrupted. On July 9, 2016 a debris flow was triggered in Fugong county of Yunnan province, and seventeen people died. The validation indicates that the results of the synthetic zonation map of DFS for the study area are in substantial agreement with both the investigation data and actual distribution of debris flows.

4.2 Conclusions

In this research, the cascade of hydropower stations region in the upper Yangtze River was selected as our case study. The early and dynamic analysis of debris flow susceptibility has been finished by analyzing the data of regional antecedent earthquakes and droughts in the region. The conclusions can be summarized as follows:

(1) This research indicates that the entire debris flow susceptibility area is 167,500km^2, of which 26,800 km^2 falls within the high susceptibility zone and 60,900 km^2 and 79,800 km^2 are in the medium and low susceptibility areas, respectively. The Baihetan, Xiangjiaba and Xiluodu hydropower stations are located within the identified risk area highly exposed to debris flows.

(2) The validation indicates that the results of the synthetic zonation map of DFS for the study

area are in substantial agreement with both the investigation data and actual distribution of debris flows. No detailed and accurate data on the DFS of cascade hydropower stations development zone in the upper Yangtze River region have been identified in previous studies. We found that the distribution of DFS is almost the same as in previous research results that the high susceptibility areas of debris flow are mainly concentrated in the southwest of Sichuan province and northwest Yunnan province.

(3) Debris flows are still likely to happen in the future based on historic examination of debris flow activities, topography, soil source and water conditions on the cascade hydropower stations development zone of the upper Yangtze River. With constant reduction of loose solid materials, the frequency and scale of some debris flow gullies will gradually reduce. However, after a strong earthquake and change of climate because of dry-wet circulation, large scale debris flows are still likely to occur in the region.

(4) The new method used in this research is exploratory and is applied for the early and dynamic analysis of DFS that combines impacts of antecedent earthquakes and droughts. The method is a unique effort amongst all different methods focusing on the early and dynamic issues of DFS due to differences of DFS with time. Based on this method, the result of DFS on the cascade hydropower stations development zone in the upper Yangtze River have potential to supply support for mitigating, assessing, controlling and monitoring debris flows hazard.

(5) It is necessary that continued analysis on the application of this method be performed in the following areas, should this method be applied in other debris flow prone basins.

Acknowledgements

We appreciated comments by anonymous reviewers on an earlier version of the manuscript. This research was supported by the National Natural Science Foundation of China (Grant No. 41661134012 and 41501012) and the Taiwan Youth Visiting Scholar Fellowship of Chinese Academy of Sciences (Grant No. 2015TW2ZB0001).

References

Bregoli F, Medina V, Chevalier G, et al. (2015) Debris-flow susceptibility assessment at regional scale: Validation on an alpine environment. Landslides 12: 437-454. https://doi.org/10.1007/s10346-014-0493-x

Cama M, Lombardo L, Conoscenti C, et al. (2017) Improving transferability strategies for debris flow susceptibility assessment: Application to the Saponara and Itala catchments (Messina, Italy). Geomorphology 288: 52-65. http://doi.org/10.1016/j.geomorph.2017.03.025

Cao Y, Hu GD (1993) Application of geographical information system at home and abroad. Ji Suan Ji Yu Xian Dai Hua 3:1-4.(in Chinese)

Carrara A, Crosta G, Frattini P (2008) Comparing models of debris-flow susceptibility in the alpine environment. Geomorphology 94: 353-378. https://doi.org/10.1016/j.geomorph. 2006.10.033

Chen NS, Yang CL, Zhou W, et al. (2009) The critical rainfall characteristics for torrents and debris flows in the Wenchuan earthquake stricken area. Journal of Mountain Science 6(4):362-372. https://doi.org/10.1007/s11629-009-1064-9

Chen NS, Deng MF, Hu GS, et al. (2010) Risk Characteristics and Prevention Strategy of Debris Flow Under the Seismic Influence in Mountainous Arid Area, Southwest China. Journal of Sichuan University (Engineering Science Edition) 42 (Supp.1): 1-6. (In Chinese)

Chen NS, Lu Y, Zhou HB, et al. (2014) Combined Impacts of Antecedent Earthquakes and Droughts on Disastrous Debris Flows. Journal of Mountain Science 11(6): 1507-1520. https://doi.org/10.1007/s11629-014-3080-7

Chen XZ, Chen H, You Y, et al. (2015) Susceptibility assessment of debris flows using the analytic hierarchy process method -A case study in Subao river valley, China. Journal of Rock Mechanics and Geotechnical Engineering 7: 404-410. https://doi.org/10.1016/j.jrmge.2015.04.003

China Earthquake Data Center (2017) http://data3.earthquake.cn/ (Accessed on 2 May 2017)

Dong JJ, Lee CT, Lin KP, et al. (2008) Debris-budget based debris-flows susceptibility analysis. Geotechnical Engineering for Disaster Mitigation and Rehabilitation. Beijing: Science Press. pp 145-151. https://doi.org/10.1007/978-3-540-79846-0-8

Du RH (1985) The research on glacial debris flow in Tibet. Sinica 4 of Lanzhou Institute of Glaciology and Cryopedology, Chinese Academy of Sciences. Beijing: Science Press. pp 1-69.

Du RH (1987) A comprehensive investigation and control planning for debris flow in the Xiaojiang River basin of Yunnan Province. 1 st. Chongqing:Science Press. pp 103-113. (In Chinese)

Fiorillo F, Guadagno FM (2012) Long karst spring discharge time series and droughts occurrence in Southern Italy. Environmental Earth Sciences 65(8): 2273-2283. https://doi.org /10.1007/s12665-011-1495-9

Han YS, Liu HJ, Zhong DL, et al. (2007) GIS-Based Risk Assessment of Debris Flow Disasters in the Upper Reach of Yangtze River. Wuhan University Journal of Natural Sciences 12(4): 657-662. https://doi.org/10.1007/s11859-006-0352-2

He N, Chen NS, Zhu YH (2013) Research on Influential Factors and Dynamic Characteristics of a Debris Flow in Aizi Gully. Journal of Hydroelectric Engineering 11(1):12-16. (In Chinese)

Hu GS, Chen NS, Wang YH, et al. (2014) Preliminary analysis of debris flow susceptibility and risk area on construction region of Baihetan hydropower station, Jinshajiang River. Earth and

Environment 42(5):652-658. (In Chinese)
Irmler R, Daut G, Mäusbacher R (2006) A debris flow calendar derived from sediments of lake Lago di Braies (N. Italy). Geomorphology 77: 69-78. https://doi.org/10.1016/j.geomorph.2006.01.013
Iverson RM, Reid ME, Logan M, et al. (2010) Positive feedback and momentum growth during debris-flow entrainment of wet bed sediment. Nature Geoscience 4: 116-121. https://doi.org/10.1038/ngeo1040
Kang ZC, Li ZF, Ma AN (2004) Debris Flows in China. Beijing: Science Press. pp 15-32. (In Chinese)
Kessler JLP, Soreghan GS, Wacker HJ (2001) Equatorial aridity in western Pangea: Lower Permian loessite and dolomitic paleosols in northeastern New Mexico, USA. Journal of Sedimentary Research 71: 817-832. https://doi.org/10.1306/2DC4096B-0E47-11D7-8643000102C1865D
Kim JH, Tsourlos P, Yi MJ, et al. (2014) Inversion of ERT data with a priori information using variable weighting factors. Journal of Applied Geophysics 105: 1-9. http://doi.org/10.1016/j.jappgeo.2014.03.003
Kritikos T, Davies T (2015) Assessment of rainfall-generated shallow landslide/debris-flow susceptibility and runout using a GIS-based approach: application to western Southern Alps of New Zealand. Landslides 12(6): 1051-1075. https://doi.org/10.1007/s10346-014-0533-6
McKee TB, Doesken NJ, Kleist J (1993) The relationship of drought frequency and duration to time scales. In: 8th conference on applied climatology, Anaheim, CA. American Meteorological Society, Boston, pp 179-184. Available online: http://ccc.atmos.colostate.edu/relationshipofdroughtfrequency.pdf (Accessed on 20 October 2013)
Li SD, Ren XS, Yue SY, et al. (2001) Earthquake and debris flow activities. Research of Soil and Water Conservation 8: 26-27. (In Chinese)
Lin CW, Shieh CL, Yuan BD (2004) Impact of Chi-Chi earthquake on the occurrence of landslides and debris flows: example from the Chenyulan River watershed, Nantou, Taiwan. Engineering Geology 71(1): 49-61. https://doi.org/10.1016/S0013-7952(03)00125-X
Liu CY (2003) Effects of earthquake on mud-rock flows. Shanxi Architecture 29(7):40-41. (in Chinese)
Liu CZ (2004) General Situation of Environmental Geology in China. Geotechnical Engineering World 7(11): 15-17. (In Chinese)
Macelloni L, Battista BM, Knapp CC (2011) Optimal filtering high-resolution seismic reflection data using a weighted-mode empirical mode decomposition operator. Journal of Applied Geophysics 75:603-614. https://doi.org/10.1016/j.jappgeo.2011.09.018
Mhaske SY, Choudhury D (2010) GIS-based soil liquefaction susceptibility map of Mumbai city for earthquake events. Journal of Applied Geophysics 70: 216-225. https://doi.org/10.1016/j.jappgeo.2010.01.001
National Meteorological Information Center (2017) Available online at: http://www.nmic.cn/web/index.htm (Accessed on 2 May 2017)
Ren JS, Wang ZX, Chen BW, et al. (1997) The New Tectonic Map of China. Regional Geology of China 16(3): 225-230. (In Chinese)
Ryan HF, Legg MR, Conrad JE (2009) Recent faulting in the gulf of Santa Catalina: San Diego to Dana Point. Earth Science in the Urban Ocean. The Southern California Continental Borderland: Geological Society of America Special Paper 454: 291-315. https://doi.org/10.1130/2009.2454(4.5)
Shi MY, Chen JP, Song Y, et al. (2015) Assessing debris flow susceptibility in Heshigten Banner, Inner Mongolia, China, using principal component analysis and an improved fuzzy C-means algorithm. Bulletin of Engineering Geology and the Environment 75(3): 909-922. https://doi.org/10.1007/s10064-015-0784-z
Tang C, Zhu J, Li WL, et al. (2009) Rainfall-triggered debris flows following the Wenchuan earthquake. Bulletin of Engineering Geology and the Environment 68(2): 187-194. https://doi.org/10.1007/s10064-009-0201-6
Tehrany MS, Pradhan B, Jebur MN (2014) Flood susceptibility mapping using a novel ensemble weights-of-evidence and support vector machine models in GIS. Journal of Hydrology 512: 332-343. https://doi.org/10.1016/j.jhydrol.2014.03.008
Veronesi F, Schito J, Grassi S, et al. (2017) Automatic selection of weights for GIS-based multicriteria decisionanalysis: site selection of transmission towers as a case study. Applied Geography 83: 78-85. https://doi.org/10.1016/j.apgeog.2017.04.001
Wang J, Yu Y, Yang S, et al. (2014) A Modified Certainty Coefficient Method (M-CF) for Debris Flow Susceptibility Assessment: A Case Study for the Wenchuan Earthquake Meizoseismal Areas. Journal of Mountain Science 11(5): 1286-1297. https://doi.org/10.1007/s11629-013-2781-7
Wang SY, Shi ZL (1993) The relationship between the sensible radius and magnitude of earthquakes and its application: The symposium on Chinese seismic zonation. Beijing: Seismological Press. pp 89-96. (In Chinese)
Wei FQ, Jiang YH, Cui P, et al. (2007) Distribution Regularity of Debris Flow and Its Hazard in Upper Reaches of Yangtze River and Other Rivers of Southwestern China. Wuhan University Journal of Natural Sciences 12(4): 619-626. https://doi.org/10.1007/s11859-006-0305-9
Wu JS, Kang ZC, Tian LQ (1990) The observation and research of debris flow in Jiangjiagou,Yunnan. Beijing: Science Press. pp 62-70. (In Chinese)
Xie H, Zhong DL, Li Y, et al. (2004) Features of debris flows in the upper reaches of the Changjiang River. Resources and environment in the Yangtze basin 13(1): 94-99. (In Chinese)
Xu WB, Yu WJ, Jing SC, et al. (2013) Debris flow susceptibility assessment by GIS and information value model in a large-scale region, Sichuan Province (China). Natural Hazards 65(3):1379-1392. https://doi.org/10.1007/s11069-012-0414-z
Yu H, Zhang DL, Wang X (2014) Application of weighted early-arrival waveform inversion to shallow land data. Journal of Applied Geophysics 102: 68-76. https://doi.org/10.1016/j.jappgeo. 2014.01.003
Yu YX, Gao MT (2001). Effects of the hanging wall and footwall on peak acceleration during the Chi-Chi Earthquake, Taiwan. Acta seismologica sinica 6: 615-621. https://doi.org/10.1007/BF02718076
Zhong DL, Xie H, Wei FQ (2010) Comprehensive regionalization of debris flow risk degree in the upper Yangtze River. Shanghai: Scientific and Technical Publishers. pp 10-40. (In Chinese)
Zhu J, Ding J, Liang JT (2011) Influences of the Wenchuan Earthquake on sediment supply of debris flows. Journal of Mountain Science 8(2): 270-277. https://doi.org/10.1007/s11629-011-2114-7
Zhu PY, Luo DF, Kou YZ (1997) Debris flow development trend of Guxiang Ravine, Xizang. Mountain Research 15: 296-299. (In Chinese).